

ARTICLE

Is the modern-day dieback of yellow-cedar unprecedented?

B.V. Gaglioti, D.H. Mann, G.C. Wiles, and N. Wiesenberg

Abstract: In Southeast Alaska, many stands of yellow-cedar (*Callitropsis nootkatensis* (D. Don) Oerst. ex D.P. Little; hereinafter "YC") contain numerous standing, dead snags. Snag-age estimates based on tree morphology have been used to support the interpretation that a warming climate after ca. 1880 has triggered unprecedented YC dieback. Here, we present new estimates of YC snag longevity by cross-dating 61 snags with morphologies that suggest they stood dead for extended periods. All but four of these snags have lost their outermost rings to decay, so we estimate when they died using a new method based on wood-ablation rates measured in six living trees that display partial cambial dieback. The results indicate that \sim 59% of YC snags that lost their branches to decay (Class 5 snags) have remained standing for >200 years, and some for as long as 450 years (snag longevity mean \pm SD: 233 \pm 92 years). These findings, along with supporting evidence from historical photos, dendrochronology, and snag-morphology surveys in the published literature suggest that episodes of YC dieback also occurred before 1880 and before significant anthropogenic warming began. The roles played by climate change in these earlier dieback events remain to be further explored.

Key words: yellow-cedar, forest decline, climate change, snag longevity.

Résumé: Dans le sud-est de l'Alaska, plusieurs peuplements de cyprès de Nootka (CN) (*Callitropsis nootkatensis* (D. Don) Oerst. ex D.P. Little) contiennent de nombreux chicots morts encore debout. L'estimation de l'âge des chicots sur la base de la morphologie a été utilisée pour appuyer l'extrapolation qu'un réchauffement du climat survenu après 1860 environ aurait déclenché un dépérissement sans précédent du CN. Nous présentons dans cet article de nouvelles estimations de la longévité des chicots du CN sur la base de la datation croisée de 61 chicots avec leurs morphologies qui indiquent qu'ils sont morts debout depuis longtemps. Tous ces chicots, à l'exception de quatre, ont perdu leurs cernes annuels les plus récents à cause de la carie du bois de telle sorte que nous estimons le moment où ils sont morts en utilisant une nouvelle méthode fondée sur le taux de perte du bois mesuré chez six arbres vivants qui présentent un dépérissement partiel du cambium. Les résultats indiquent qu'environ 59 % des chicots de CN qui ont perdu leurs branches à cause de la carie (chicots de classe 5) sont restés debout pendant plus de 200 ans, et certains jusqu'à 450 ans (longévité moyenne des chicots \pm écart-type : 233 \pm 92 ans). Ces résultats, avec des preuves à l'appui provenant de vieilles photos, de la dendrochronologie et de relevés morphologiques des chicots dans des articles publiés, indiquent que des épisodes de dépérissement du CN sont aussi survenus avant 1880 et avant qu'un réchauffement climatique significatif d'origine anthropique débute. Les rôles joués par le changement climatique dans le cas de ces épisodes antérieurs de dépérissement nécessitent d'être étudiés davantage. [Traduit par la Rédaction]

Mots-clés: cyprès de Nootka, dépérissement des forêts, changement climatique, longévité des chicots.

1. Introduction

1.1. Background on yellow-cedar decline

Yellow-cedar (*Callitropsis nootkatensis* (D. Don) Oerst. ex D.P. Little; hereinafter "YC") is an economically and culturally important tree species that is experiencing high rates of growth decline and mortality in northwestern North America's temperate rainforest (Fig. 1a) (Shaw et al. 1985; Hennon 1986; Hennon et al. 1990a, 2012). Yellow-cedar dieback is thought to begin with the freezing and loss of fine roots, which is followed by the development of root lesions that expand to the lower bole, then by cambial death, browning of foliage, and finally tree death (Hennon 1986). At present, mapped YC dieback zones with abundant snags cover ~3000 km² between the middle coast of British Columbia (~50.9°N)

and northern Chichagof Island, Alaska (\sim 57.9°N) (Hennon 2005; Hennon et al. 2016).

Significant evidence supports the current paradigm explaining YC dieback as an effect of recent climate change; specifically, that YC trees are dying because recent warming has caused an increase in the frequency and (or) the intensity of thaw events during late winter. The idea here is late-winter thaws remove the insulating snowpack, which causes shallow YC roots to deharden during warm intervals, which then makes the fine roots vulnerable to damage during subsequent frost events (Hennon et al. 2012, 2016). Direct support for this fine-root, frost-damage hypothesis (FRFD) includes experimental evidence showing that YC is more likely than co-occurring conifer species to de-harden during warm periods in late winter and early spring, and therefore

Received 8 January 2021, Accepted 26 August 2021,

B.V. Gaglioti. Water and Environmental Research Center, Institute of Northern Engineering, University of Alaska Fairbanks, Fairbanks, Alaska 99775, USA; Lamont-Doherty Earth Observatory of Columbia University, Palisades, New York 10964, USA.

D.H. Mann. Institute of Arctic Biology, University of Alaska, Fairbanks, Alaska 99708, USA.

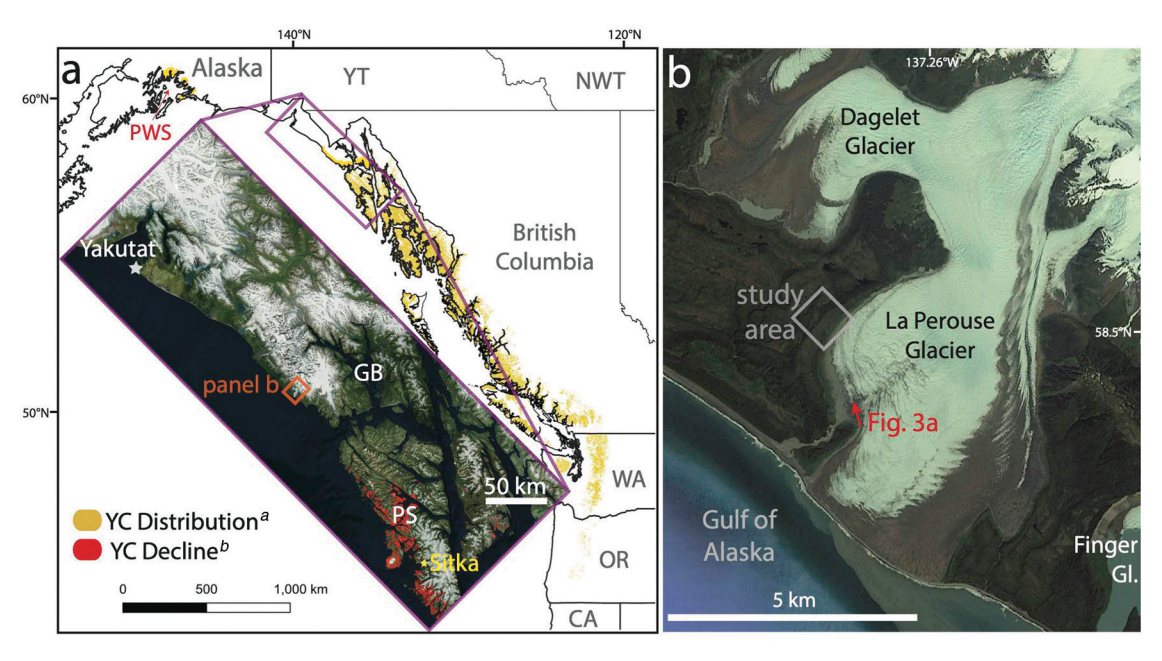
G.C. Wiles. Department of Earth Sciences, The College of Wooster, Wooster, Ohio 44691, USA; Lamont-Doherty Earth Observatory of Columbia University, Palisades, New York 10964, USA.

N. Wiesenberg. Department of Earth Sciences, The College of Wooster, Wooster, Ohio 44691, USA.

Corresponding author: B.V. Gaglioti (email: bvgaglioti@alaska.edu).

© 2021 The Author(s). Permission for reuse (free in most cases) can be obtained from copyright.com.

Fig. 1. (a) Current range of yellow-cedar is shown by yellow shading (^aBuma et al. 2017). Inset shows cumulative yellow-cedar decline in red as mapped in 2010 (^bhttps://catalog.data.gov/dataset/yellow-cedar-decline-cumulative-survey-20102) overlying Bing.com/maps satellite imagery. PWS, Prince William Sound; GB, Glacier Bay; PS, Peril Strait, where Hennon et al. (1990b) estimated snag longevity. (b) La Perouse study area. Red arrow indicates the direction of the view shown in Fig. 3a, and gray box outlines the area where we sampled forest-plots and yellow-cedar snags. [Colour online.]



that YC is more likely to suffer from root damage during subsequent cold events (Schaberg et al. 2008, 2011). One source of indirect support for the FRFD hypothesis comes from observations that dieback zones are largely confined to the middle of YC's range distribution mostly on low- to mid-elevation, south-facing slopes (Buma et al. 2017). Such sites experience large winter and spring temperature fluctuations and so are places where a warming climate is most likely to cause reduced snow insulation, which may then expose de-hardened roots to sub-zero temperatures (Hennon et al. 1990a, 2012; D'Amore and Hennon 2006; Wooton and Klinkenberg 2011).

1.2. Dating the onset of yellow-cedar decline

Previous studies suggest that YC decline began ca. 1880, coincident with the onset of post-Little Ice Age (CE 1250–1850; LIA) warming and with a presumed increase in the frequency and (or) intensity of winter thaw events in Southeast Alaska (Hennon and Shaw 1994). Two lines of evidence are used to support this 1880 starting time. (i) Dying and dead YC trees in Southeast Alaska were mentioned by explorers only after ca. 1880 (Hennon 1986), which assumes that the existence of dead and dying cedars would have been recorded by earlier explorers visiting the region. (ii) Existing estimates of YC snag longevity indicate that the oldest snags (Class 5; Fig. 2) in dieback zones died after ca. 1880 (Hennon et al. 1990b). Therefore, snag-abundant forests are assumed to represent post-LIA dieback.

Hennon et al. (1990b) used two methods to estimate how long it takes for different YC snag morphologies to develop in the forests of Southeast Alaska. Their first method used the timing of growth releases in western hemlock (*Tsuga heterophylla* (Raf.) Sarg.) trees growing next to YC snags to infer when the snags died. The idea here is that the hemlock tree benefited from increases in light and nutrients after the adjacent YC tree died, triggering enhanced radial growth rates in the hemlock (Fraver and White 2005; Stan and Daniels 2010). The second method used by Hennon et al. (1990b) to estimate the age of YC snags was to assign ages to the dead portions of otherwise live YC. YC trees frequently experience partial

cambial death or "strip-bark morphology", which results in vertically oriented strips of living tissue that continue to lay down annual rings despite partial death of the tree's canopy and trunk. By linking the dieback year recorded in these strip-bark trees with the morphology of the trees' dead tops, Hennon et al. (1990b) assigned a range of years-since-death to different snag morphologies (Fig. 2). This system of estimating dieback age is based on YC trees in the Peril Strait area ("PS" in Fig. 1a), and it has been used to date the onset (ca. 1880) and expansion (ca. 1925) of YC dieback throughout Southeast Alaska and British Columbia (Hennon et al. 1990a, 2016; D'Amore and Hennon 2006; Stan et al. 2011; Wooton and Klinkenberg 2011; Oakes et al. 2014; Bisbing et al. 2019; Comeau et al. 2019).

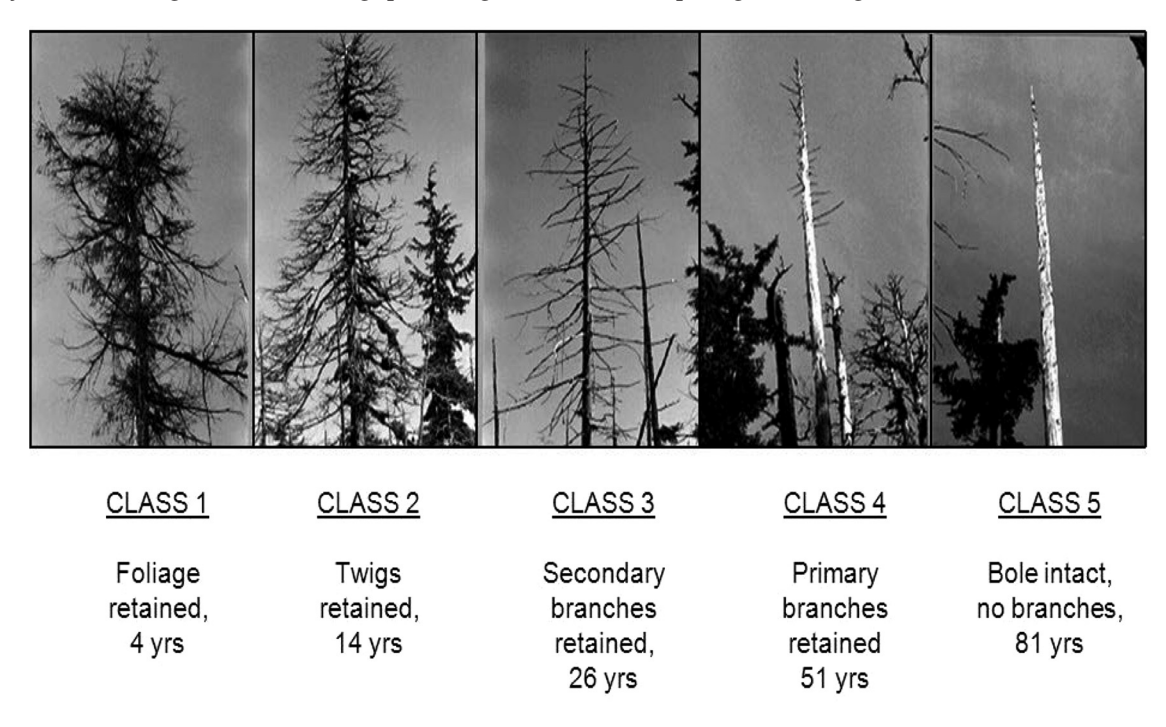
1.3. Building on Hennon's snag-aging methods

The age of older-looking YC snags (Classes 4 and 5) has not been thoroughly assessed since the pioneering work of Hennon et al. (1990b) (but see Stan et al. 2011). Further quantification of YC snag longevity is needed because old-looking snags are numerous in today's YC dieback zones (discussed in Section 5.2.2 below), and more accurate estimates of when they died can determine whether today's post-1880 YC decline is historically unprecedented and associated with anthropogenic warming. If prehistoric YC dieback events did occur, then they would serve as useful case studies to better understand the previous climatic causes and possible future trajectories of the current dieback event. In this paper, we use dendrochronology and stand-composition surveys to estimate the longevity of YC snags to test the hypothesis that Class 5 snags represent only trees that have died since ca. 1880.

2. Study area

Extensive YC stands containing numerous snags occur on glacial moraines formed over the last several thousand years on the foreland of the La Perouse Glacier along the outer coast of Glacier Bay National Park and Preserve (Figs. 1, 3). Vegetation consists of coastal temperate rainforest (Figs. 3*b*–3*c*), and the climate is hyper-maritime, with a mean annual precipitation of 3.9 m and

Fig. 2. Classification categories for yellow-cedar snags with their distinguishing morphological characteristics and mean estimated years since death (figure from Hennon et al. (2016) based on data from Hennon et al. (1990b), and reprinted with permission from the author). In this study, we focus on age estimates of snags possessing Class 4 and 5 morphologies standing near La Perouse Glacier.



mean July and January temperatures of 12.4 and -2.1 °C, respectively, at sea level in Yakutat, Alaska, 180 km to the northwest of La Perouse Glacier (Fig. 1a) (Arguez et al. 2012). In addition to old-growth YC stands growing outside of the LIA glacial limit (Figs. 3a, 3c), we discovered YC snags in a sub-fossil "ghost" forest that was exhumed from beneath the glacier's retreating terminus ca. 2015 (Fig. 3d). Previous cross-dating of these trees indicates that they were overrun by outwash gravels aggrading in front of the advancing La Perouse Glacier ca. CE 1862 (Gaglioti et al. 2019a). Wood and sometimes bark are well-preserved in this ghost forest, which allows tree identification to the genus level. Both the living forest and the ghost forest contain numerous, older YC snags (Classes 4 and 5) described by Hennon et al. (1990b) (Fig. 2). The US Forest Service has been responsible for mapping YC dieback in the last 35 years, and using these field observations, they now consider the La Perouse forests as the northernmost known YC stand exhibiting evidence of past dieback (Figs. 1a, 3b–3c) (https://www.fs.usda.gov/detailfull/r10/forest-grasslandhealth/? cid=FSEPRD538720&width=full; 2019 Update).

3. Methods

3.1. Field collections

We identified and measured every living tree and dead snag with a diameter at breast height of >5 cm (DBH; \sim 1.2 m above ground) inside four 30 m \times 30 m plots on the La Perouse Glacier's moraine complex (Figs. 1b, 3a). We collected tree cores (0.5 mm diameter) from 67 randomly selected and living YC trees at three sites (Porcupine Pond, Shin Boku, and View Terrace; Fig. 2). Cross-sections were taken at heights of 20 to 100 cm above root crown from 74 YC snags. These included 35 still-standing snags in the ghost forest that, due to the presence of a furrowed bole margin, suggest that they had already been dead when aggrading outwash gravels buried them ca. CE 1862 (Gaglioti et al. 2019a), as well as 39 standing snags in the living forest outside of the LIA ice limit (Figs. 3c, 4). We also collected cross-sections from six, recently living trees displaying partial cambial dieback ("strip-

bark morphology") from the areas around La Perouse and Finger Glaciers (Figs. 1, 5). These trees (hereinafter referred to as "ablation-estimator trees") were used to estimate post-death ablation rates (rate of wood decayed and lost) from the dead portions of the bole margins (see Section 3.2.3 below).

3.2. Data analysis

3.2.1. Estimating the longevity of yellow-cedar snags relative to other conifer species using forest plot surveys

Forest plot data was used to calculate a Snag Persistence Index (SPI) describing the longevity of YC snags compared to the standing dead snags of other conifer species. The SPI is calculated by dividing the ratio of YC snags to non-YC snags by the ratio of live YC trees to live non-YC within the same plot. An SPI of >1 suggests that YC snags are over-represented relative to their representation among living trees because of greater snag longevity. A meaningful SPI relies on the assumption that the species composition of the forest has not changed significantly over time.

3.2.2. Tree-ring analysis

We sanded tree cores and cross-sections with progressively finer sandpaper up to 1200 grit to reveal ring boundaries. Ring widths were measured to 0.001 mm either manually using a Velmex stage Quick Check counter and the program MeasureJ2X, or digitally using high-resolution scans uploaded to the computer program CooRecorder 8.1. Undated ring-width series from dead snags were visually and statistically cross-dated to their outermost preserved ring in interfurrow margins using standard dendrochronological techniques (Holmes 1983; Stokes and Smiley 1996). A master chronology was built by first detrending individual series with a negative exponential curve and then obtaining the bi-weight robust mean of individual ring-width indices. For cross-dating, we used only the time period when the reference chronology had an Expressed Population Statistic (EPS) of >0.85, which is the interval of sufficient replication in the chronology to reflect forest-wide patterns of tree growth (Wigley et al. 1984).

Fig. 3. (a) Photograph of study area including La Perouse Glacier and sites where forest surveys and dendrochronological sampling were done (MC, moraine crest; VT, View Terrace; SB, Shin Boku; PP, Porcupine Pond). The maximum extent of the La Perouse Glacier was reached in CE 1895, in the latter part of the Little Ice Age (LIA) (Gaglioti et al. 2019a). Note person in bottom right for scale. (b) Class 4 and 5 yellow-cedar snags near the View Terrace forest plot with the La Perouse Glacier in the background. (c) Old-growth forest on the late Holocene moraine complex as viewed from near the ice edge. Note the numerous yellow-cedar snags (gray trunks). (d) A portion of the ghost forest that was overrun by the advancing La Perouse Glacier ca. CE 1862 and exhumed in 2015 as the glacier retreated (Gaglioti et al. 2019a). [Colour online.]

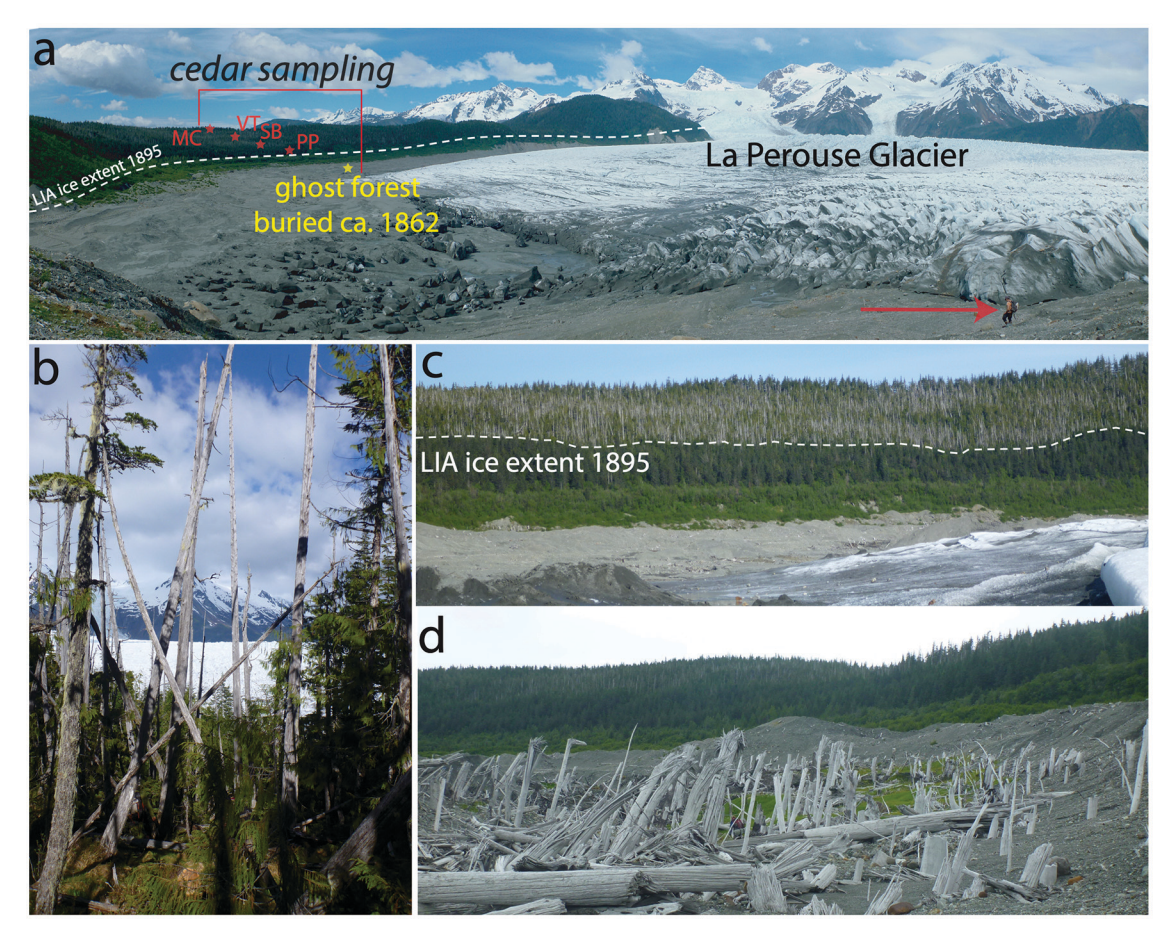
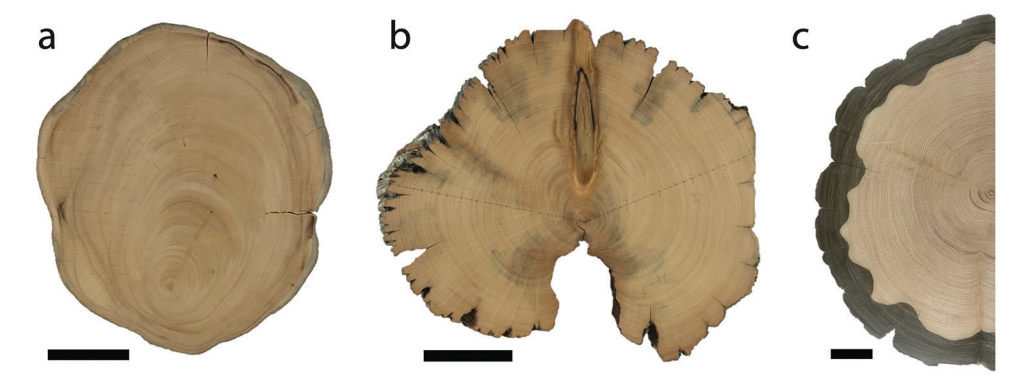


Fig. 4. Cross-sections of yellow-cedar snags collected near La Perouse Glacier. (a) A standing, Class 4 snag that retained its sapwood and an outermost ring (Sample VT3). (b) A furrowed Class 5 snag that has lost its sapwood following a period of outer-ring ablation after tree death (Sample SB7). (c) A portion of a ghost forest tree that was a standing dead snag at the time of burial (Sample BF26). The dark stain lining the outer margin was caused by waterlogging when the ghost forest was buried by outwash gravels and ice (ca. 1862–2015). Scale bars are 5 cm. [Colour online.]

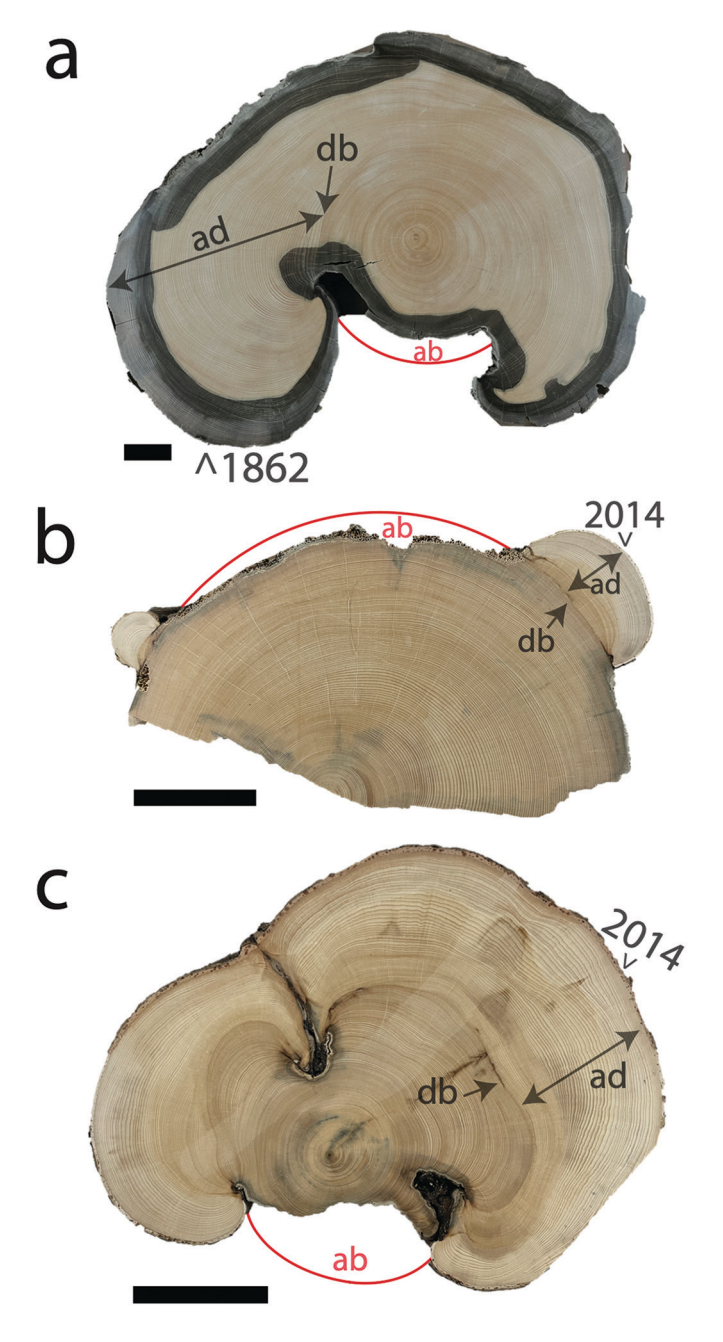


Snags were considered "cross-dated" when their ring-width series had significant (p < 0.05) interseries correlations and shared marker years with the master chronology. Cross-dating was verified using the COFECHA software (Holmes 1983) and the *dplr* package for the R studio program (Bunn 2008).

3.2.3. Estimating outer-ring ablation rates of yellow-cedar snags

To accurately estimate the year of death of individual snags that have lost their outer rings, we must estimate the amount of outer wood ablated since tree death and the number of rings lost in that ablated wood. We first quantified ablation rates from six

Fig. 5. Three of the six ablation-estimator trees used to estimate ablation rates in yellow-cedar snags. ad, ablation duration; db, ring representing dieback year; red line, former bole margin at the time of dieback; ab, shows the amount of ablation. The ablation rate calculation is shown in Fig. 6. (a) This scarred tree was alive when buried under glacial outwash ca. CE 1862 (Sample BF8). (b) Strip-bark tree from Porcupine Pond site whose cambium had partially died back in CE 1899 and was killed in a windthrow in 2014 (Sample CC22). (c) Partial-dieback tree from Porcupine Pond site with a dieback date of CE 1900 and was killed in a windthrow in 2014 (Sample CC25). Scale bars are 5 cm. [Colour online.]



ablation-estimator trees (Fig. 5). We used these observed ablation rates to estimate the number of rings lost after each tree died. To do this, we first transformed tree ring-width series from all cross-sections with an intact pith into a time series of basal area increments (BAI) (mm²/year; the "inside-out method") (Biondi and

Qeadan 2008). This was done to estimate how growth and ablation rates affected the total area of wood in a given cross-section over time. We used the BAI measurement (mm²/year) instead of "radius lost" (mm/year) because the radius measurement does not account for the fact that snags with larger diameters have lower rates of outer-ring loss (ablation) than those of smaller diameter snags (Graham and Cromack 1982). For example, if the ablation rate is calculated from a change in radius, then 2 cm of outer-ring ablation would occur at the same rate for all snag sizes; however, the corresponding change in cross-sectional area would be greater for a large-diameter snag relative to a smalldiameter snag. For example, a snag decreasing in diameter from 75 to 73 cm decreases in basal area by 5809 mm², while a smaller snag decreasing from 20 to 18 cm in diameter decreases in basal area by only 1492 mm². More time is needed to ablate the greater area on the larger snag; therefore, using the change in BAI provides more realistic estimates of outer-ring ablation rates for snags of differing diameters.

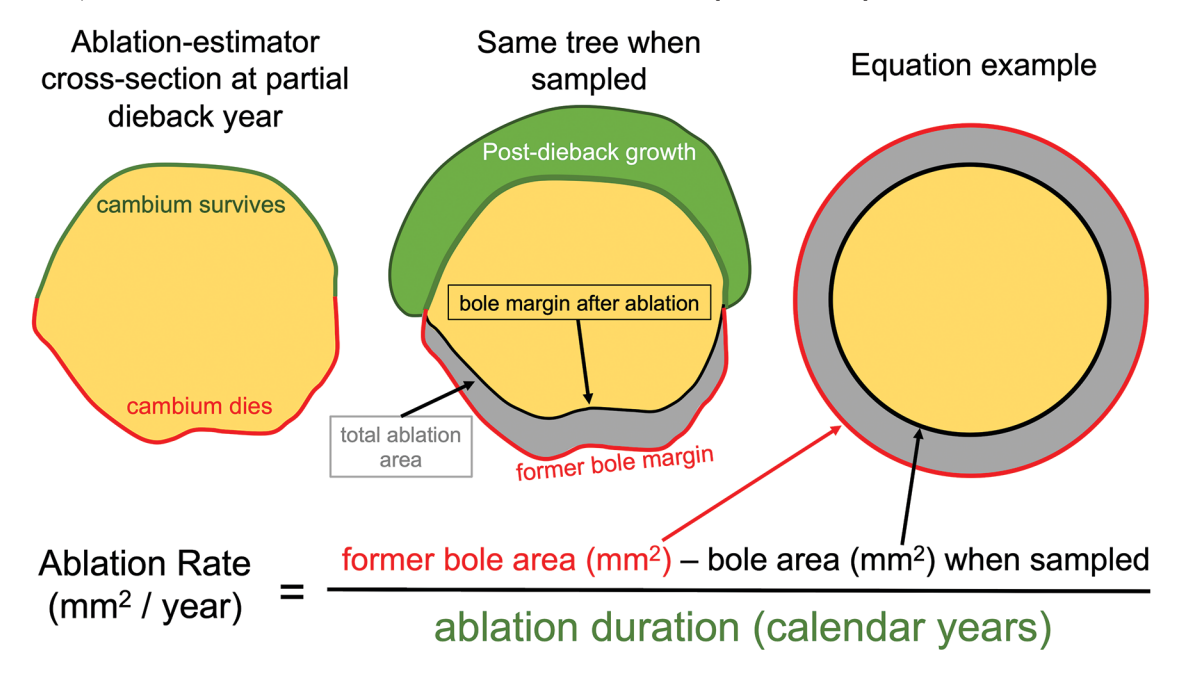
Calendar-dated rings in the cross-sections of ablation-estimator (strip-bark) trees provide three key pieces of information needed to estimate ablation rates in YC snags: (i) the year of partial cambial dieback in the intact portion of the stem ("db" in Fig. 5, dark green line in Fig. 6); (ii) the amount of wood lost from the dieback margin ("ab" in Fig. 5, gray area in Fig. 6), which is calculated by subtracting the area of a circle outlining the outermost dieback zone from a circle outlining the scarred ring; and (iii) the length of time over which ablation occurred ("ablation duration"), which is obtained using the outer-ring calendar year minus the calendar year of the dieback scar (ablation duration: "ad" in Fig. 5). We made these measurements on the six ablation-estimator trees in order to obtain a range of ablation rates that could be applied to cedar snags that had lost their outer rings, with the goal of estimating how much wood was lost through ablation after these snags had died (mm²/year of wood lost from the outer margin of a cedar snag; equation shown in Fig. 6).

3.2.4. Estimating the year of death for partially ablated snags

To estimate when a snag died, we use an iterative process in which succeeding years' worth of wood ablation (between 59 and 111 mm²/year, as determined from the six ablation-estimator trees) are added onto the outermost preserved margin of a snag ("ablation add-ons") (Figs. 7a–7b). Then, by using the mean and a 95% confidence-interval range of the annual BAI for the 100 outermost rings preserved in the snag ("preserved rings" in the yellow areas in Figs. 5, 7), we calculate how many annual rings would be contained in each ablation-increment add-on (called "lost rings" as shown in Figs. 7a–7b). Because we know the calendar year of the outermost preserved ring of each snag based on cross-dating, we also know the calendar year of each lost ring contained within the ablation add-ons, and thus can estimate the calendar year of tree death for each iteration of ablation add-on.

Using these converging estimates of tree growth and wood decay, we then calculate the number of years that each snag would have experienced ablation of its outermost rings ("ablation duration") following each iteration of ablation-increment add-on (Figs. 7b, 7c). Ablation duration is calculated by subtracting the calendar year of the outermost lost ring from the year of sampling (or year of burial in the case of the ghost forest trees; CE 1862). For example, in the case of the non-ghost-forest trees, the ablation duration is the sampling year (2018), minus the estimated calendar year of the outermost lost ring for each add-on iteration. For each snag, the estimated year of tree death is the calendar year of the outermost lost ring when the ablation duration equals the number of ablation-increment add-ons. In other words, the outermost, possible, add-on ring represents the calendar year when the ablation duration prior to sampling agrees with how much time this wood would have likely taken to ablate.

Fig. 6. Post-death, outer-wood ablation rates in yellow-cedar snags can be estimated using strip-bark trees whose boles exhibit partial cambial dieback. (Left) Cross-section of a YC tree at the time of partial cambial dieback. (Middle) The same cross-section several years later when sampled. This includes the post-dieback ablation area (gray), and the areas where annual rings continued to be added during the post-dieback growth period (green). (Right) We used the area of a circle outlining both the pre- and post-ablation bole margins to calculate the total ablation area. We then divided this total ablation area by the number of years in the post-dieback growth period (ablation duration) to estimate the ablation rates for six ablation-estimator trees. [Colour online.]



Three separate iterative processes of reverse ablation were applied to each snag to constrain the range of potential snag longevities (dashed and solid lines in Fig. 7c). The *maximum* snag longevity estimate used the fastest ablation rate (111.2 mm²/year) observed in the six strip-bark trees, coupled with an extrapolated (lost ring) growth rate based on the 5th percentile of BAI of the 100 outermost rings preserved in that particular snag (i.e., the thinnest rings). The *minimum* snag longevity was estimated using the slowest ablation rates observed in the six strip-bark trees (59.3 mm²/year) coupled with extrapolated rings based on the BAI of the 95th percentile of the rings preserved in the snag. The *midrange* longevity estimate was based on the mean ablation rate (87.4 mm²/year) observed in the ablation-estimator trees in conjunction with the mean BAI of the 100 outermost rings preserved in the snag in question.

4. Results

4.1. Forest plot data and the cedar snag persistence index

Cedar snags comprise 56% and 37% of the basal area of all YC trees in the three living-tree plots and in the ghost-forest plot, respectively (Table 1). The SPI (Snag Persistence Index) at the Porcupine Pond site could not be calculated due to the absence of non-cedar snags. Thus, we excluded this site from our overall SPI estimates because the forest composition at that location has probably changed in the recent past. At the other three sites, YC snags are 4.4 to 7.5 times more abundant than what would be predicted based on the species composition of the living trees (Fig. 8). Therefore, we estimate that dead cedars stand 4.4 to 7.5 times longer than non-cedar snags (combined sites SPI: 6.9).

All sampled snags outside the ghost forest had "mature" snag morphologies, meaning that they either retained only a few primary branches (n = 1, Class 4 snag) or were branchless poles (n = 29, Class 5 snags; Hennon et al. 1990b; Figs. 2, 3b). The majority of unsampled dead cedars on the Holocene moraine complex were

also Class 4 and 5 snags (Figs. 2, 3*b*, 3*c*). Overall, there was minimal evidence of recent dieback in the La Perouse Glacier area.

4.2. Cedar tree-ring chronology and snag cross-dating

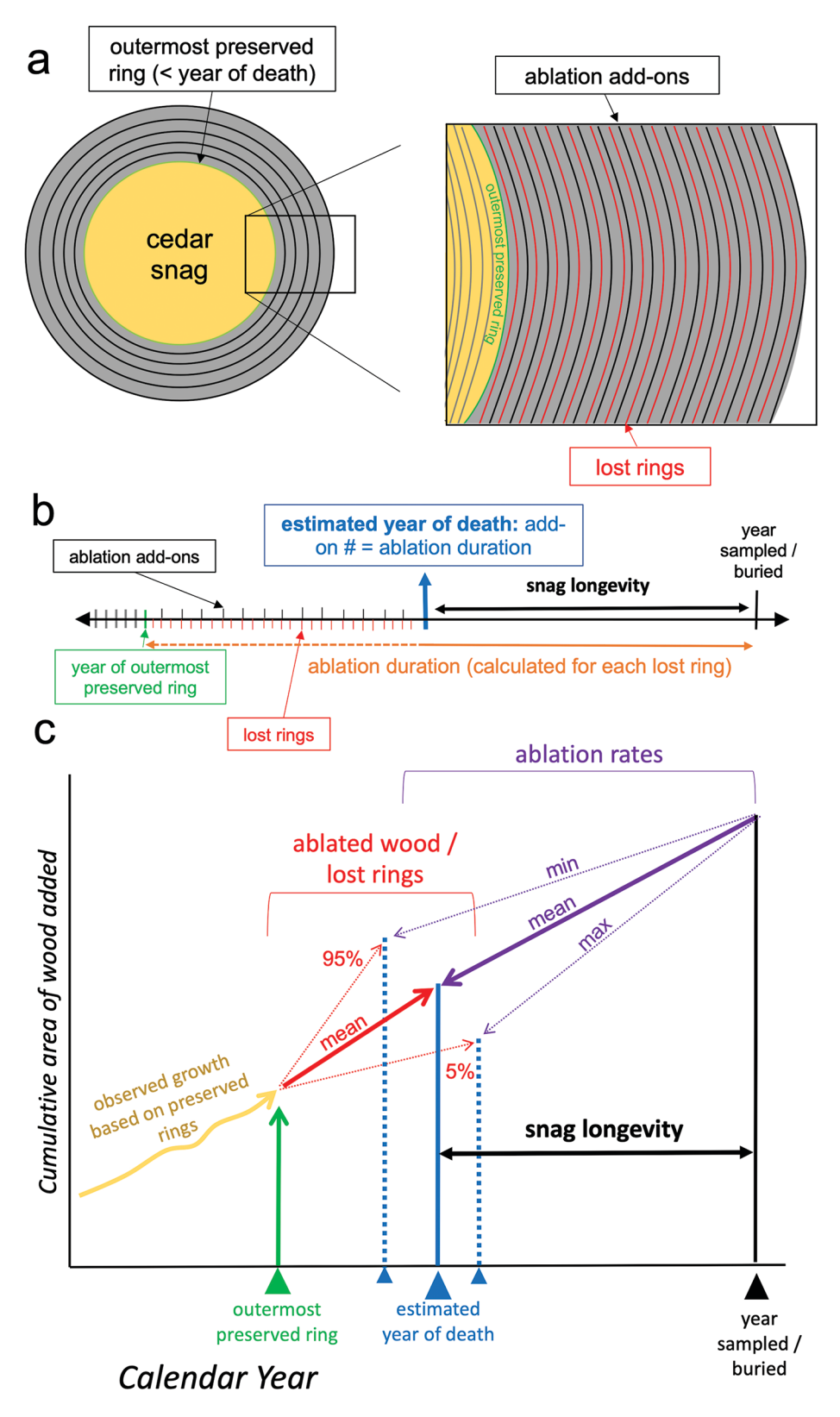
The YC tree-ring chronology from the La Perouse Glacier area consists of 244 ring-width series from 164 trees (Fig. 9). One hundred and twenty-nine of these series are from 67 living trees, and 30 of these series are from 29 snags sampled from the living forest (Fig. 3a; Gaglioti et al. 2019a). Eighty-three ring-width series (from 68 trees) are from the ghost forest buried by glacial outwash ca. CE 1862. Of these, 51 series (36 trees) were alive when buried (including one strip-bark tree), and 32 series (32 trees) had died prior to burial (they were already snags when the glacier arrived). The outermost rings of 13 snags could not be cross-dated due to extremely tight growth.

The master chronology from the YC sampled at the La Perouse Glacier foreland spans the period CE 1138 to 2018 (881 years) with a mean interseries correlation of 0.40. The portion of the chronology with an EPS of >0.85 spans the period from CE 1388 to 2017 (630 years) (Fig. 9). Individual series' correlations between the 61 snags that had cross-dated outer rings and the master chronology have a mean of 0.37 (range: 0.13–0.54; p value range: 0.00–0.12) (Table 2). We include the cross-dated calendar ages for three snags with interseries correlation p values of >0.05 because they share exceptionally narrow rings following volcanic cooling events with the same marker years in the master chronology (i.e., CE 1696, 1770, 1810; Fig. 9). The calendar years of the preserved outer rings in snags range from CE 1450 to 1936 (Fig. 10a).

4.3. When does sapwood ablation occur in yellow-cedar snags?

The three ghost-forest snags that retained their sapwood and still had intact outer rings had been standing dead for 22, 24, and 35 years before they were buried ca. CE 1862 (starred samples in Table 2), with two of these snags containing the burrows of wood-boring beetles (c.f., Cerambycidae). Another ghost-forest snag

Fig. 7. Conceptual figure describing the ablation add-on method for estimating the year of tree death for cross-dated yellow-cedar snags that have experienced outer-ring ablation. (a) Succeeding years of ablation are added back onto the outermost preserved margin of a snag, based on the observed ablation rates in six, strip-bark, ablation-estimator trees (Figs. 5, 6). Included in this ablation add-on is the estimated number of lost rings based on the mean and 95%-range of ring-widths still preserved in the snag (rings measured in yellow area). (b) For every iteration of ablation add-on, we calculate the ablation duration based on the sampling year minus the calendar year represented by the outermost lost ring. The most likely year of death is the calendar year of the outermost lost ring when the estimated ablation duration equals the number of ablation add-ons. (c) Overview of the method showing the three ablation rates and growth rates used in estimating snag death. [Colour online.]



Can. J. For. Res. Downloaded from cdnsciencepub.com by CASA Institution Identity on 12/02/21 For personal use only.

Fable 1. Forest plot data showing the composition of live trees and dead snags within four 30 m imes 30 m plots.

									Cedar:		Cedar:	0,	Snag	
									other live		other	I	preservation	on
									count ratio	- 1	snag ratio		ndex^p	
	Latitude	Latitude Longitude Elevation	Elevation		No. of live trees	No. of live trees Total DBH (cm) No. of dead	No. of dead	Total DBH (cm)						
Site name	(°N)	(w)	(m)	Species ^a	>5 cm DBH	of live trees	snags >5 cm DBH	of dead snags	Count	DBH	Count DBH Count DBH		Count DBH	BH
Moraine Crest (MC) 58.50012 137.304	58.50012	137.304	235	Alaska yellow-cedar 40	40	978	15	483	2	2.39	15	27	7.5	11.29
				Hemlock	20	409	1	18						
View Terrace (VT) 58.49737 137.306817 228	58.49737	137.306817	228	Alaska yellow-cedar	45	473	20	349	1.5	0.84	29.9	10.26	4.44	12.21
				Western hemlock	11	113	2	12						
				Mountain hemlock	28	446	1	22						
				Sitka spruce	1	4	0	0						
Japanese Garden (JG) 58.49902 137.302617 181	58.49902	137.302617	181	Alaska yellow-cedar	51	989	29	1030	1.59	1.6	11.16	69.9	7	4.17
				Western hemlock	26	260	2	52						
				Mountain hemlock	5	134	3	26						
				Sitka spruce	1	က	1	2						
Porcupine Pond (PP) 58.49858 137.301568 158	58.49858	137.301568	158	Alaska yellow-cedar	29	428	48	1426	0.28	0.3	48^{c} 1	1426^{c} 1	168.82 4917	917
				Western hemlock	64	802	0	0						
				Sitka spruce	38	641	0	0						

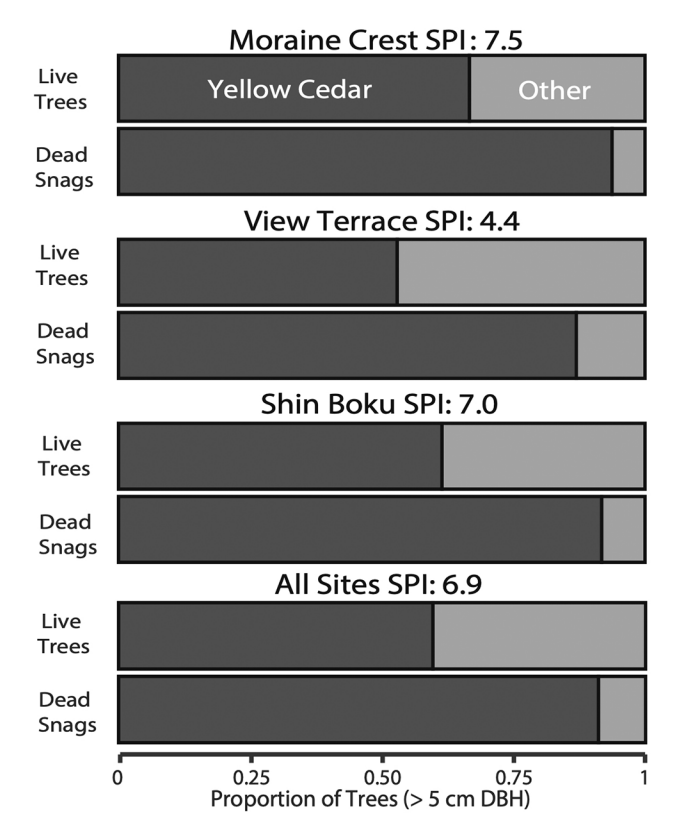
Note: DBH, diameter at breast height.

Scientific Latin names: Alaska yellow cedar, Callitropsis nootkatensis; hemlock, Tsuga spp.; western hemlock Tsuga heterophylla; mountain hemlock, Tsuga mertensiana; Sitka spruce, Picea sitchensis

There were no dead non-cedar trees in these plots, so these ratios represent minimums.

Fig. 8. Forest composition of yellow-cedar snags relative to hemlock (*Tsuga* spp.) and Sitka spruce (*Picea sitchensis*). The yellow-cedar Snag Persistence Index (SPI) represents the ratio of yellow-cedar to non-cedar snags relative to the ratio of living yellow-cedar trees to living non-yellow-cedar trees. These data suggest that dead yellow-cedar trees tend to remain standing as snags for 4.4 to 7 times longer than other conifer species growing at the same site.

Can. J. For. Res. Vol. 51, 2021



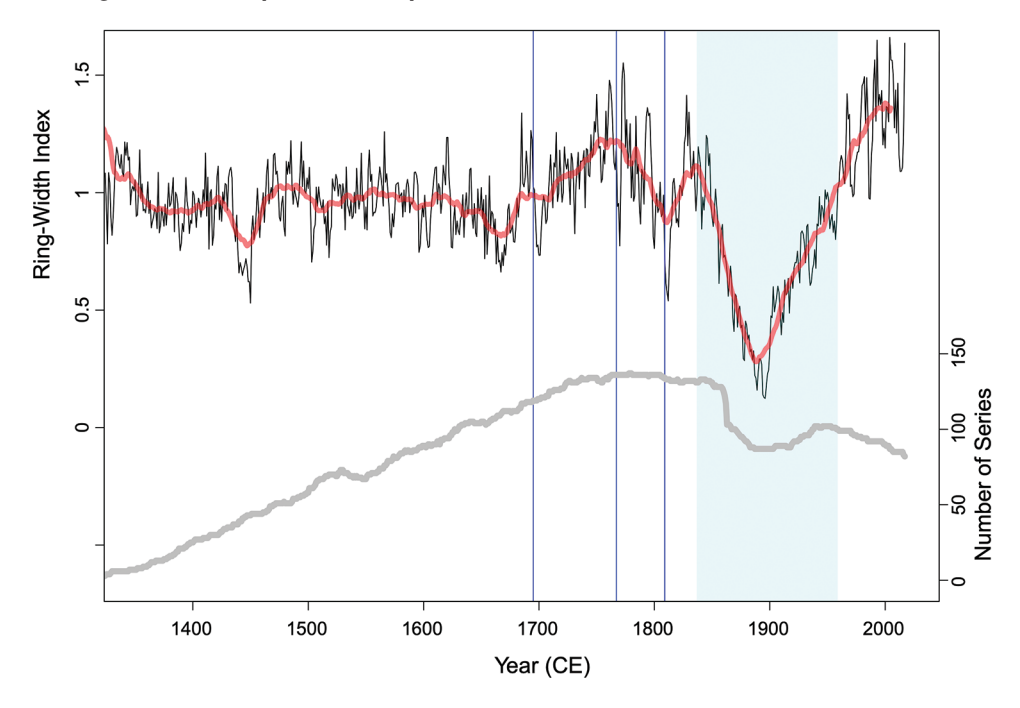
with partially degraded sapwood had an outer ring date of CE 1758, which means this snag lost a portion of its sapwood while standing for <104 years (buried: CE 1862). The one Class 4 snag sampled from the living forest that retained all its sapwood had an outermost ring dating to CE 1936 (Fig. 4a; "VT3" in Table 2) (sampled in 2018; standing for 82 years). In summary, evidence indicates that YC sapwood can remain intact for up to 82 years after tree death with sapwood ablation in progress at <104 years following tree death.

4.4. Estimated calendar year of snag death

The outer-ring ablation-rate estimates derived from the six, ablation-estimator trees range from 59 to 111.2 mm²/year (mean: 89.5 mm²/year). In terms of the radius of a large-sized YC snag, this means that a 75-cm-diameter bole would be reduced by 0.076 mm diameter/year if we use the mean observed ablation rate from the six ablation-estimator trees. If the outer rings ablated at the average rate (89.5 mm²/year), and the lost rings were of an average thickness, then the estimated number of rings lost from the 61 snags ranges from 11 to 183 years (mean \pm SD: 55 ± 42) (Table 2).

YC snags that have lost their branches and some of their outer rings have remained standing after death for an average of 233 years (SD: 93 years) (Fig. 10). The full range of estimated, minimum snag longevity spans 27 to 466 years (Table 2). Even using the most conservative estimate (thinnest 5th percentile of a tree's preserved ring-widths and the fastest observed ablation rate), we estimate that snags that have lost their branches (Class 5)

Fig. 9. Yellow-cedar tree-ring chronology from the La Perouse Glacier foreland. The running 20-year mean is shown in red, and the number of tree-ring series contributing to the record is shown by the gray line below. Vertical dark-blue lines mark the onset of volcanic cooling events that triggered reduced cedar growth and resulted in thin marker years. Blue box shows when the advancing glacier caused localized cooling and cedar growth decline. [Colour online.]



may have stood, on average, for at least 169 years (SD: 82) and for a maximum of 382 years after they died (Table 2). All longevity estimates of <80 years represent a minimum estimate of snag longevity because limited evidence suggests that sapwood degradation is not underway until 80–100 years after death (see Section 4.3), and most of the samples used to estimate rates of sapwood loss had lost at least some of their sapwood. All estimates of snag lifespans are minimum-limiting ones because all the snags we sampled were probably destined to remain standing for many more years, based on the fact that even the oldest snags we felled had undecayed heartwood and were still firmly rooted. In summary, of the 57 Class 5 snags we sampled in the La Perouse area, 80% had been standing for longer than 140 years before being either buried by glacial outwash in CE 1862 or being sampled by us in 2018.

5. Discussion

5.1. Yellow-cedar snag longevity

Our snag longevity estimates (Fig. 10) add to the Hennon et al. (1990b) snag morphology rubric (Fig. 2). Our one direct date of a Class 4 snag dying 82 years ago (based on a preserved outer-ring) is within the range suggested by Hennon et al. (1990b) of 24 to 100 years (mean \sim 51 years; Fig. 2). However, the range of Class 5 snag-longevity estimates we present here (mean \pm SD: 233 \pm 92) is significantly greater than what Hennon et al. (1990b) estimated (mean \sim 81 years; Fig. 2). We estimate that most (\sim 59%) Class 5 snags on the La Perouse Glacier foreland have remained standing for >200 years after they died (Fig. 10c; Table 2), and furthermore that snag morphology often does not change markedly 80–100 years after a YC tree dies (also observed in Hennon et al. 2000).

Snag-age estimates from other studies support our finding that Class 5 YC snags can stand for >140 years, the time required for them to represent dieback that occurred before 1880. Stan et al. (2011) describes a Class 5 YC snag near Prince Rupert, British Columbia that stood 279 years after death and retained its outermost

ring. Similarly, the oldest YC snags cross-dated in two separate studies on Vancouver Island died 157 years (Parish and Antos 2004) and approx. 200 years before sampling (Kellner et al. 2000).

The longevity of western red cedar (*Thuja plicata* Donn ex D.Don) snags is relevant here because, like YC, its wood is highly resistant to decay, and the two species inhabit similar climatic zones (Hennon 1991; Hennon et al. 1999). Daniels et al. (1997) showed that red cedar snags can stand for >270 years after death and concluded that morphology-based snag-age classes are not reliable indicators of the timing of tree death in older-looking snags. In addition, some of the red cedar trees killed by ground subsidence during the Cascadia Earthquake in CE 1700 still stand as snags in Washington (Yamaguchi et al. 1997). The fact that red and YC snags can remain standing for centuries in a wide range of climatic zones make it unlikely that the periglacial microclimate near the La Perouse Glacier has significantly increased the longevity of YC snags in our study area.

5.2. Did yellow-cedar dieback occur before 1880?

5.2.1. Competing hypotheses

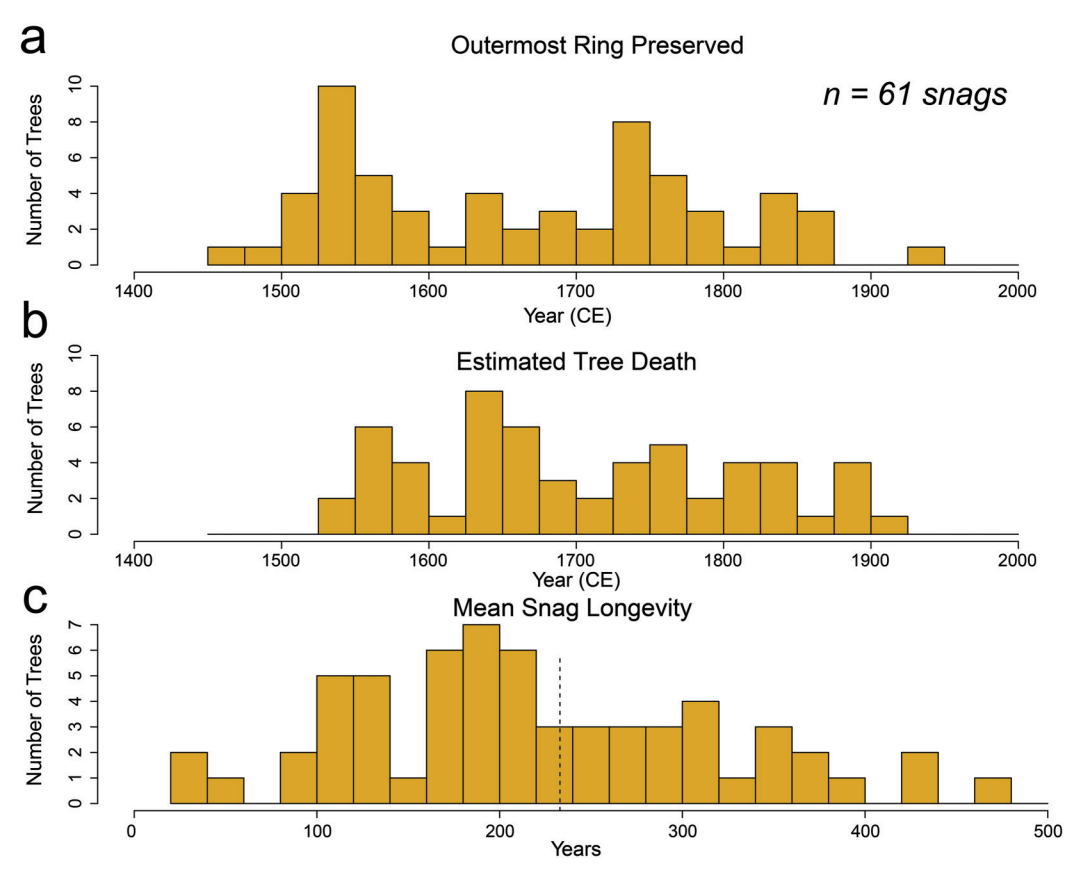
Here we refer to the hypothesis that YC decline is exceptional to modern times beginning ca. 1880 as the *modern-day exceptionalism* (MDE) hypothesis (Hennon et al. 1990b, 2016; Krapek et al. 2017). The MDE has been widely accepted in the YC literature and assumes that YC dieback seldom occurred during the LIA because the climate was colder then and late-winter thaw periods were less frequent (Hennon and Shaw 1994; Hennon et al. 2012, 2016). The alternative suggested by our findings is that many Class 5 snags standing in dieback zones actually date to pre-1880 dieback events that occurred prior to the end of the LIA and before the onset of significant post-LIA and anthropogenic warming in this region (Hegerl et al. 2007; Wiles et al. 2014). We call this the "It happened before" (IHB) hypothesis. Several predictions stem from the IHB hypothesis that can be tested using existing data.

Table 2. Cross-dating and year of tree death estimates for 61 snag samples.

				Lost rii	ngs		Death	year		Snag ye	ar since de	ath
Sample name	Series correlation with master	Correlation p value	Outermost preserved ring	Mean	Lower	Upper	Mean	Lower	Upper	Mean	Lower	Upper
BF03	0.43	0	1689	12	28	5	1701	1717	1694	161	145	162
BF05	0.43	0	1536	15	32	8	1551	1568	1544	311	294	315
BF07	0.44	0	1523	27	64	12	1550	1587	1535	312	275	32
BF11	0.37	0	1542	25	60	12	1567	1602	1554	295	260	302
BF12	0.48	0	1627	15	38	6	1642	1665	1633	220	197	226
BF13	0.32	0	1696	30	74	12	1726	1770	1708	136	92	148
BF14	0.37	0	1735	12	23	6	1747	1758	1741	115	104	118
BF17	0.35	0	1584	16	44	7	1600	1628	1591	262	234	267
BF18 BF19	0.15	0.0143	1538 1534	137	277	51 70	1675	1815	1589	187	47	250
BF19 BF20	0.16 0.54	0.0216 0	1534	147 99	296 184	70 50	1681 1641	1830 1726	1604 1592	181 221	32 136	231 248
BF22*	0.43	0	1835	NA	NA	NA	NA	NA	NA	27	NA	NA
BF25	0.33	0	1587	60	117	28	1647	1704	1615	215	158	234
BF29	0.18	0.0115	1675	11	38	4	1686	1713	1679	176	149	180
BF30	0.48	0.0115	1530	63	151	31	1593	1681	1561	269	181	286
BF32	0.42	0	1652	36	67	19	1688	1719	1671	174	143	182
BF34	0.43	0	1737	19	51	7	1756	1788	1744	106	74	114
BF34 (2)	0.4	0	1726	15	43	7	1741	1769	1733	121	93	126
BF35	0.33	0	1612	18	32	9	1630	1644	1621	232	218	236
BF41	0.46	0	1495	38	298	12	1533	1793	1507	329	69	348
BF42	0.4	0	1627	21	48	9	1648	1675	1636	214	187	221
BF45*	0.44	0	1834	NA	NA	NA	NA	NA	NA	28	NA	NA
BF47	0.38	0	1646	26	84	11	1672	1730	1657	190	132	199
BF53	0.23	0.0016	1524	50	142	19	1574	1666	1543	288	196	310
BF55*	0.45	0	1821	NA	NA	NA	NA 1760	NA 1770	NA 1764	41	NA	NA
BF57	0.26	0	1758	11	21	6	1769	1779	1764	93	83	96
BF58 BF60	0.42 0.25	0.0001	1643 1574	16 43	42 94	8 18	1659 1617	1685 1668	1651 1592	203 245	177 194	207 261
BF61	0.13	0.0559	1535	22	74	9	1557	1609	1544	305	253	313
BF62	0.48	0.0333	1727	17	32	8	1744	1759	1735	118	103	122
BF65	0.28	0.0001	1530	43	78	21	1573	1608	1551	289	254	300
CC1	0.46	0	1778	59	101	29	1837	1879	1807	181	139	211
CC2	0.37	0	1747	93	162	41	1840	1909	1788	178	109	230
CC3	0.46	0	1553	31	107	13	1584	1660	1566	434	358	452
CC4	0.31	0	1790	49	87	25	1839	1877	1815	179	141	203
CC5	0.42	0	1589	59	123	24	1648	1712	1613	370	306	405
CC6	0.37	0	1837	37	67	16	1874	1904	1853	144	114	165
SB1	0.54	0	1728	45	110	19	1773	1838	1747	245	180	271
SB10	0.13	0	1793	98	142	57	1891	1935	1850	127	83	168
SB11	0.37	0	1558	104	215	51	1662	1773	1609	356	245	409
SB12 SB13	0.24	0.0003 0	1771 1509	71 150	158 297	30 70	1842 1659	1929 1806	1801 1579	176 359	89 212	217 439
SB13 (2)	0.34 0.46	0	1864	16	30	70 8	1880	1894	1872	138	124	439 146
SB13 (2) SB14	0.38	0	1858	29	69	12	1887	1927	1870	131	91	148
SB14 (2)	0	0.0004	1568	107	184	49	1675	1752	1617	343	266	401
SB2a	0.52	0.0001	1741	42	77	21	1783	1818	1762	235	200	256
SB2b	0.17	0.0004	1555	152	328	59	1707	1883	1614	311	135	404
SB3	0.31	0	1762	56	114	30	1818	1876	1792	200	142	226
SB4	0.36	0	1686	68	122	32	1754	1808	1718	264	210	300
SB4 JG	0.39	0	1523	29	113	11	1552	1636	1534	466	382	484
SB5a	0.34	0	1546	45	131	16	1591	1677	1562	427	341	456
SB5b	0.5	0	1751	67	156	27	1818	1907	1778	200	111	240
SB6	0.43	0	1763	57	115	28	1820	1878	1791	198	140	227
SB7	0.43	0	1704	58	119	24	1762	1823	1728	256	195	290
SB8	0.43	0	1462	183	312	75 52	1645	1774	1537	373	244	481
SB9	0.42	0	1527	107	219	53	1634	1746	1580	384	272	438
VT10 VT12	0.43 0.39	0	1831 1732	69 68	124 180	38 26	1900 1800	1955 1912	1869 1758	118 218	63 106	149 260
V112 VT3*	0.39	0.0161	1732 1936	NA	NA	NA	1800 NA	1912 NA	1/58 NA	82 82	NA	NA
VT7	0.36	0.0101	1710	103	224	44	1813	1934	1754	205	84	264
VT8	0.47	0	1856	61	104	32	1917	1960	1888	101	58	130
	,	-					_					
Average	0.36		1666	55 193	120	25 75	1708	1773	1678	233	169	260
Max. Min.	0.54		1936 1462	183	328	75 4	1917 1533	1960 1568	1888 1507	466	382	484
IVIIII.	0		1462	11	21	4	1533 107	1568	1507	93	32	96

Note: Samples followed by an asterisk (*) had a preserved outermost ring that represented the last year of growth, so the year of tree deaths and snag longevity estimates were not adjusted by outer-ring ablation rates. Summary stats for death years in the final row are for Class 5 snags only.

Fig. 10. (a) Outermost preserved ring (20-year age bins) in 61 cross-dated yellow-cedar snags from the moraine forest sampled in 2018 and the ghost forest buried ca. CE 1862. (b) Mean estimated year of tree death based on the ablation add-on method using mean rates of ablation and lost-ring growth. (c) Longevity estimates for cross-dated snags based on the outermost preserved rings adjusted using the mean observed ablation rates and mean ring width in the snags. Vertical line marks the mean of snag longevity for the 57 cross-dated Class 5 snags whose outer rings had been lost to post-death ablation. [Colour online.]



5.2.2. Predictions of the It happened before hypothesis

IHB prediction No. 1: Class 5 snags that potentially represent pre-1880 dieback events are common in declining YC stands

Hennon (1986) found that Class 5 snags comprised 8%-60% of all YC snags at 23 forest plots exhibiting active dieback. At one site (Patterson Bay) that lacked any evidence of modern dieback, the only snags present were "long-dead Class 4 and 5 snags". Oakes et al. (2014) described vegetation in 50 forest plots in Southeast Alaska and found that Class 5 snags make up 12%, 10%, and 23% of all YC snags at sites that exhibit recent, mid-range, and old cedar decline, respectively, and one site in a northerly location dominated by Class 5 snags with almost no modern dieback, which is similar to the situation in the La Perouse study area. D'Amore and Hennon (2006) surveyed 132 vegetation plots in YC stands on Chichagof and Baranof Islands and found that Class 5 snags made up \sim 7% to \sim 57% of all snags (mean: 22%). At the La Perouse Glacier study site, Class 5 snags make up the vast majority of dead YC trees, and account for 56% and 37% of the basal area of all YC and all standing conifer trees, respectively. The available evidence indicates that Class 5 snags, which we show often represent pre-1880 dieback events (Fig. 10b), comprise a significant proportion of the dead trees observed in surveyed YC dieback zones.

IHB prediction No. 2: Expanding YC dieback zones were initiated prior to $1880\,$

This prediction can be partially tested with data presented by Hennon et al. (1990b), who used aerial imagery collected in 1927,

1948, and 1976 to quantify the expansion rates of seven YC dieback zones on Chichagof and Baranof Islands. We can extend this approach by using the mean expansion rates that Hennon et al. (1990b) estimated for the 20th century to estimate the size of the same die-back zones further back in time, specifically when they would have measured one hectare in size. This back-calculation approach suggests that six out of seven measured dieback zones would have initiated prior to 1880 (Table 3), which is consistent with the IHB hypothesis.

IHB prediction No. 3: Even Class 5 snags that died shortly after 1880 require a pre-1880 dieback mechanism because they started declining well before they died

When trees die of abiotic factors unrelated to sudden disturbance events, they typically show signs of compromised vigor over several decades (Cailleret et al. 2017). Hennon et al. (1990b) reported that most YC strip-bark trees experienced reduced growth for ~50 years prior to the onset of partial cambial dieback. Comeau et al. (2019) also found that YC experiencing the initial symptoms of dieback exhibited reduced growth for several decades before being sampled. We sampled only one Class 4 snag (VT3) on the La Perouse Glacier foreland that can be used to test this prediction because it has retained its outermost ring. The ring-width series of VT3 indicates that this tree experienced a significant growth decline starting ~30 years before it eventually died in 1936. The implication for these pre-death growth declines is that even the older Class 5 snags post-dating 1880 reported in Hennon et al. (1990b) probably started to decline well before this

Table 3. Inception age of seven yellow-cedar dieback zones reported in Hennon et al. 1990b.

		Rate of expansion (ha/year)						
Site	Size in 1927 (ha)	1927–1948 1948–1965		1965–1976	Mean expansion rate	Years needed to reach 1927 size	Estimated inception year	Estimated inception year if zone began as 1 ha
AP1	22	0.29	0.37	0.4	0.35	62	1865	1868
AP2	1.1	0.02	0.06	0.09	0.06	19	1908	1925
AP3	22.4	0.12	0.13	0.11	0.12	187	1740	1749
AP4	18.3	0.11	0.04	0.04	0.06	289	1638	1654
AP5	19.8	0.08	0.16	0.1	0.11	175	1752	1761
AP6	33.7	0.39	0.24	0.21	0.28	120	1807	1810
AP7	60.3	0.2	0.32	0.24	0.25	238	1689	1693
Average	_	_	_	_	_	_	1771	1780

Note: These calculations were made by extrapolating the rate of growth observed between 1927 and 1976 back to before 1927 to determine the year of dieback initiation if the dieback zone began as a 1 ha area.

time. Again, this conclusion is consistent with what the IHB hypothesis predicts.

IHB prediction No. 4: The warm winters causing YC dieback during the 20th century also occurred episodically during the LIA

Winter climate in Southeast Alaska is intimately tied to the Pacific Decadal Oscillation (PDO) and to the strength of the Aleutian Low Pressure system (AL) (Hartmann and Wendler 2005). A strong AL leads to a positive phase of the PDO, which is accompanied by relatively warm, rainy winters in Southeast Alaska that likely enhance YC dieback on a regional scale (Hennon et al. 2016; Hartmann and Wendler 2005; Wendler et al. 2016). Based on what we currently know about the dynamics of the AL/PDO over the last 500 years from paleoclimate records, it is likely that the warm winters thought to be driving YC decline in recent times were preceded by similar periods during the long and climatically variable LIA period (Anderson et al. 2005; Osterberg et al. 2017; Bailey et al. 2018; Gaglioti et al. 2019b). The LIA was not a 650-year interval of uniformly cold winter climate in Southeast Alaska as suggested by the MDE hypothesis; instead it encompassed multiple warmer and colder episodes.

IHB prediction No. 5: Other tree species also experienced pulses of recruitment and death during the LIA, indicating that LIA-recruitment pulses in YC trees were not unique

Evidence for recruitment pulses occurring before 1880 has been used to infer that YC was predisposed to benefit from the cold LIA climate (Hennon et al. 2016; Krapek et al. 2017). However, pulses of recruitment also occurred in mountain hemlock (Wiles et al. 2014; Gaglioti et al. 2019b), Sitka spruce (Barclay et al. 2001), and shore pine (Sullivan et al. 2015) during the LIA in Southeast Alaska. Because widespread tree recruitment occurred in all major tree species during the LIA, the observation that mature, living YC germinated during a 650-year period prior to 1900 should not be used as evidence for a "healthier" YC population existing at that time. Instead, pulses of YC recruitment during the LIA were probably a matter of chance (after all, the LIA was both long and recent), and in any case the existence of LIA-aged recruitment pulses does little to preclude the occurrence of pre-1880 dieback events. In contrast, isolated stands of YC near Juneau, Alaska were rapidly expanding during the LIA, and have become relatively stable during the post-1900 period, a pattern which supports the MDE hypothesis (Krapek et al. 2017).

5.3. Summarizing support for the IHB hypothesis

Evidence for pre-1880 dieback events in today's YC stands include (i) the presence of Class 5 snags that potentially have stood dead for centuries; (ii) estimates of the initiation dates of modern dieback zones based on hindcast, pre-1927 expansion trajectories; and (iii) the fact that a multi-decadal growth decline

commonly precedes YC death in Class 5 snags that died after 1880. Another important point is that the occurrence of YC recruitment pulses during the LIA does not preclude the occurrence of pre-1880 dieback events. Finally, in contrast to the predictions of the modern-day-exceptionalism hypothesis, the LIA was not a period of monotonously cold winters that provided unwavering refuge for warm-sensitive YC trees.

Although the IHB hypothesis is consistent with the data presented here and in the existing literature, we do not yet know whether YC age cohorts represent cycles of regeneration, which, centuries later could result in cohorts of similarly aged snags, and (or) if they result from region-wide episodes of mortality driven by climatic cycles. The idea of episodic climatic stress is basically what Hennon and co-workers have inferred, and testing this idea further into the past is the next step in understanding the ecology of this remarkable tree species. To better understand the trajectory of the current YC dieback event, we need paleoenvironmental data that describes the climates and site conditions that accompanied pre-1880 dieback events.

6. Conclusions

Snag-longevity data from the northernmost known stands of YC exhibiting past dieback shed new light on questions surrounding the unprecedented nature of ongoing YC dieback in Southeast Alaska and British Columbia. We find that in YC stands on the La Perouse Glacier foreland, snags make up 56% of yellowcedar basal area and probably persist after death \sim 7 times longer than hemlock and Sitka spruce trees. We describe a new method (the ablation-add-on method) that uses dendrochronology to estimate the calendar year when a partially decayed YC snag died. This method works by forward-extrapolating annual growth rates measured in the wood that is still preserved in the snag's interior until it meets the backwards-extrapolated, outer-ring ablation rates. Using this method, we find that 57 Class 5 yellow-cedar snags, which according to earlier, morphology-based estimates of snag age would have been estimated to have died 50-128 years ago, in fact died 93-466 years ago with a snag lifespan of at least 233 \pm 93 years (mean \pm SD). This exceptional longevity of YC snags suggests that many morphologically old snags, which are common in yellow-cedar dieback zones elsewhere, are likely to have died during dieback episodes occurring prior to the advent of significant post-LIA warming, which previous workers have suggested as an underlying cause of YC dieback. More work is now needed to identify the links between prehistoric YC dieback events and paleoclimate changes.

Acknowledgements

This project was funded by the National Science Foundation Paleoclimate Program (P2C2-2002561 and 2002454). We thank

Phillip Wilson, Ned Rozell, Andy Paonessa, and Lewis Sharman for their help in the field. Our thinking about yellow-cedar ecology benefitted from discussions with Greg Streveler, Paul Hennon, Lauren Oakes, and John Krapek. Constructive review comments by Lori Daniels and two anonymous reviewers helped improve this manuscript. Transportation was provided by Hans Munich of Yakutat Coastal Airlines, and we benefitted from logistical support by John Gates of Red-Roof B&B, Yakutat. Glacier Bay National Park and Preserve permitted this work.

References

- Anderson, L., Abbott, M.B., Finney, B.P., and Burns, S.J. 2005. Regional atmospheric circulation change in the North Pacific during the Holocene inferred from lacustrine carbonate oxygen isotopes, Yukon Territory, Canada. Quat. Res. 64(1): 21–35. doi:10.1016/j.yqres.2005.03.005.
- Arguez, A., Durre, I., Applequist, S., Vose, R.S., Squires, M.F., Yin, X., et al. 2012. NOAA's 1981–2010 US climate normals: an overview. Bull. Am. Meteorol. Soc. 93(11): 1687–1697. doi:10.1175/BAMS-D-11-00197.1.
- Bailey, H.L., Kaufman, D.S., Sloane, H.J., Hubbard, A.L., Henderson, A.C., Leng, M.J., et al. 2018. Holocene atmospheric circulation in the central North Pacific: a new terrestrial diatom and $\delta^{18}O$ dataset from the Aleutian Islands. Quat. Sci. Rev. 194: 27–38. doi:10.1016/j.quascirev.2018.06.027.
- Barclay, D.J., Calkin, P.E., and Wiles, G.C. 2001. Holocene history of Hubbard Glacier in Yakutat Bay and Russell Fiord, southern Alaska. Geol. Soc. Am. Bull. 113(3): 388–402. doi:10.1130/0016-7606(2001)113<0388:HHOHGI>2.0.CO;2.
- Biondi, F., and Qeadan, F. 2008. A theory-driven approach to tree-ring standardization: defining the biological trend from expected basal area increment. Tree-Ring Res. **64**(2): 81–96. doi:10.3959/2008-6.1.
- Bisbing, S.M., Buma, B.J., Oakes, L.E., Krapek, J., and Bidlack, A.L. 2019. From canopy to seed: loss of snow drives directional changes in forest composition. Ecol. Evol. 9(14): 8157–8174. doi:10.1002/ece3.5383. PMID:31380079.
- Buma, B., Hennon, P.E., Harrington, C.A., Popkin, J.R., Krapek, J., Lamb, M.S., et al. 2017. Emerging climate-driven disturbance processes: widespread mortality associated with snow-to-rain transitions across 10° of latitude and half the range of a climate-threatened conifer. Global Change Biol. 23(7): 2903–2914. doi:10.1111/gcb.13555.
- Bunn, A.G. 2008. A dendrochronology program library in R (dplR). Dendrochronologia, 26(2): 115–124. doi:10.1016/j.dendro.2008.01.002.
- Cailleret, M., Jansen, S., Robert, E.M., Desoto, L., Aakala, T., Antos, J.A., et al. 2017. A synthesis of radial growth patterns preceding tree mortality. Glob. Change Biol. 23(4): 1675–1690. doi:10.1111/gcb.13535.
- Comeau, V.M., Daniels, L.D., Knochenmus, G., Chavardès, R.D., and Zeglen, S. 2019. Tree-rings reveal accelerated yellow-cedar decline with changes to winter climate after 1980. Forests, 10(12): 1085. doi:10.3390/f10121085.
- D'Amore, D.V., and Hennon, P.E. 2006. Evaluation of soil saturation, soil chemistry, and early spring soil and air temperatures as risk factors in yellow-cedar decline. Glob. Change Biol. 12(3): 524–545. doi:10.1111/j.1365-2486.2006.01101.x.
- Daniels, L.D., Dobry, J., Klinka, K., and Feller, M.C. 1997. Determining year of death of logs and snags of *Thuja plicata* in southwestern coastal British Columbia. Can. J. For. Res. **27**(7): 1132–1141. doi:10.1139/x97-055.
- Fraver, S., and White, A.S. 2005. Identifying growth releases in dendrochronological studies of forest disturbance. Can. J. For. Res. 35(7): 1648–1656. doi:10.1139/x05-092.
- Gaglioti, B.V., Mann, D.H., Wiles, G.C., Jones, B.M., Charlton, J., Wiesenberg, N., and Andreu-Hayles, L. 2019a. Timing and potential causes of 19th-century glacier advances in coastal Alaska based on tree-ring dating and historical accounts. Front. Earth Sci. 7: 82. doi:10.3389/feart.2019.00082.
- Gaglioti, B.V., Mann, D.H., Williams, A.P., Wiles, G.C., Stoffel, M., Oelkers, R., et al. 2019b. Traumatic resin ducts in Alaska mountain hemlock trees provide a new proxy for winter storminess. J. Geophys. Res. Biogeosci. 124(7): 1923–1938. doi:10.1029/20181G004849.
- Graham, R.L., and Cromack, K., Jr. 1982. Mass, nutrient content, and decay rate of dead boles in rain forests of Olympic National Park. Can. J. For. Res. 12(3): 511–521. doi:10.1139/x82-080.
- Hartmann, B., and Wendler, G. 2005. The significance of the 1976 Pacific climate shift in the climatology of Alaska. J. Clim. **18**(22): 4824–4839. doi:10.1175/JCLI3532.1.
- Hennon, P.E. 1986. Pathological and ecological aspects of decline and mortality of Chamaecyparis nootkatensis in southeast Alaska. University of Oregon Dissertation.
- Hennon, P.E. 1991. Persistence of western hemlock and western red cedar trees 38 years after girdling at cat island in southeast Alaska. US Department of Agriculture, Forest Service, Pacific Northwest Research Station, Vol 507
- Hennon, P.E. 2005. Yellow-cedar decline in the north coast forest district of British Columbia. US Department of Agriculture, Forest Service, Pacific Northwest Research Station Vol. 549.
- Hennon, P., and Shaw, C., III. 1994. Did climatic warming trigger the onset and development of yellow-cedar decline in southeast Alaska. Forest Pathol. 24(6–7): 399–418. doi:10.1111/j.1439-0329.1994.tb00833.x.

- Hennon, P., Hansen, E., and Shaw, C., III. 1990a. Dynamics of decline and mortality of *Chamaecyparis nootkatensis* in southeast Alaska. Can. J. Bot. 68(3): 651–662. doi:10.1139/b90-085.
- Hennon, P., Shaw, C., III, and Hansen, E. 1990b. Dating decline and mortality of *Chamaecyparis nootkatensis* in southeast Alaska. For. Sci. **36**(3): 502–515.
- Hennon, P.E., McClellan, M.H., and Palkovic, P. 1999. Comparing deterioration and ecosystem function of decay-resistant and decay-susceptible species of dead trees. US Department of Agriculture Forest Service General Technical Report PSW-GTR-181.2002.
- Hennon, P.E., Wittwer, D.T., Stevens, J., and Kilborn, K. 2000. Pattern of deterioration and recovery of wood from dead yellow-cedar in southeast Alaska. West. J. Appl. For. 15(2): 49–58. doi:10.1093/wjaf/15.2.49.
- Hennon, P.E., D'Amore, D.V., Schaberg, P.G., Wittwer, D.T., and Shanley, C.S. 2012. Shifting climate, altered niche, and a dynamic conservation strategy for yellow-cedar in the North Pacific coastal rainforest. BioScience, 62(2): 147–158. doi:10.1525/bio.2012.62.2.8.
- Hennon, P.E., McKenzie, C.M., D'Amore, D., Wittwer, D.T., Mulvey, R.L., Lamb, M.S., et al. 2016. A climate adaptation strategy for conservation and management of yellow cedar in Alaska. US Department of Agriculture, Forest Service, Pacific Northwest Research Station.
- Hegerl, G.C., Crowley, T.J., Allen, M., Hyde, W.T., Pollack, H.N., Smerdon, J., and Zorita, E. 2007. Detection of human influence on a new, validated 1500-year temperature reconstruction. J. Clim. 20(4): 650–666. doi:10.1175/JCLI4011.1.
- Holmes, R.L. 1983. Computer-assisted quality control in tree-ring dating and measurement. Tree-Ring Bull. 43: 69–78.
- Kellner, A.M., Laroque, C.P., Smith, D.J., and Harestad, A.S. 2000. Chronological dating of high-elevation dead and dying trees on northern Vancouver Island, British Columbia. Northwest Sci. 74(3): 242–247.
- Krapek, J., Hennon, P.E., D'Amore, D.V., and Buma, B. 2017. Despite available habitat at range edge, yellow-cedar migration is punctuated with a past pulse tied to colder conditions. Divers. Distrib. 23(12): 1381–1392. doi:10.1111/ ddi.12630.
- Oakes, L.E., Hennon, P.E., O'Hara, K.L., and Dirzo, R. 2014. Long-term vegetation changes in a temperate forest impacted by climate change. Ecosphere, 5(10): 1–28. doi:10.1890/ES14-00225.1.
- Osterberg, E.C., Winski, D.A., Kreutz, K.J., Wake, C.P., Ferris, D.G., Campbell, S., et al. 2017. The 1200-year composite ice core record of Aleutian Low intensification. Geophys. Res. Lett. 44(14): 7447–7454. doi:10.1002/2017GL073697.
- Parish, R., and Antos, J.A. 2004. Structure and dynamics of an ancient montane forest in coastal British Columbia. Oecologia, 141(4): 562–576. doi:10.1007/s00442-004-1690-4. PMID:15322898.
- Schaberg, P.G., Hennon, P.E., D'Amore, D.V., and Hawley, G.J. 2008. Influence of simulated snow cover on the cold tolerance and freezing injury of yellow-cedar seedlings. Glob. Change Biol. 14(6): 1282–1293. doi:10.1111/j.1365-2486.2008.01577.x.
- Schaberg, P.G., D'Amore, D.V., Hennon, P.E., Halman, J.M., and Hawley, G.J. 2011. Do limited cold tolerance and shallow depth of roots contribute to yellow-cedar decline? For. Ecol. Manage. 262(12): 2142–2150. doi:10.1016/j.foreco.2011.08.004.
- Shaw, C., III, Laurent, T., and Hennon, P.E. 1985. Decline and mortality of Chamaecyparis nootkatensis in southeastern Alaska, a problem of long duration but unknown cause. Plant Dis. 69(1): 13–17.
- Stan, A.B., and Daniels, L.D. 2010. Calibrating the radial-growth averaging method for detecting releases in old-growth forests of coastal British Columbia, Canada. Dendrochronologia, 28(3): 135–147. doi:10.1016/j.dendro. 200910.003
- Stan, A.B., Maertens, T.B., Daniels, L.D., and Zeglen, S. 2011. Reconstructing population dynamics of yellow-cedar in declining stands: Baseline information from tree rings. Tree-Ring Res. 67(1): 13–25. doi:10.3959/2009-7.1.
- Stokes, M.A., and Smiley, T.L. 1996. An introduction to tree-ring dating. University of Arizona Press.
- Sullivan, P.F., Mulvey, R.L., Brownlee, A.H., Barrett, T.M., and Pattison, R.R. 2015. Warm summer nights and the growth decline of shore pine in Southeast Alaska. Environ. Res. Lett. 10(12): 124007. doi:10.1088/1748-9326/10/12/124007.
- Wendler, G., Galloway, K., and Stuefer, M. 2016. On the climate and climate change of Sitka, Southeast Alaska. Theor. Appl. Climatol. 126(1–2): 27–34. doi:10.1007/s00704-015-1542-7.
- Wigley, T.M., Briffa, K.R., and Jones, P.D. 1984. On the average value of correlated time series, with applications in dendroclimatology and hydrometeorology. J. Climate Appl. Meteor. 23(2): 201–213. doi:10.1175/1520-0450 (1984)023<0201:OTAVOC>2.0.CO;2.
- Wiles, G.C., D'Arrigo, R.D., Barclay, D., Wilson, R.S., Jarvis, S.K., Vargo, L., and Frank, D. 2014. Surface air temperature variability reconstructed with tree rings for the Gulf of Alaska over the past 1200 years. The Holocene, 24(2): 198–208. doi:10.1177/0959683613516815.
- Wooton, C.E., and Klinkenberg, B. 2011. A landscape-level analysis of yellow-cedar decline in coastal British Columbia. Can. J. For. Res. 41(8): 1638–1648. doi:10.1139/x11-061.
- Yamaguchi, D.K., Atwater, B.F., Bunker, D.E., Benson, B.E., and Reid, M.S. 1997. Tree-ring dating the 1700 Cascadia earthquake. Nature, **389**(6654): 922–923. doi:10.1038/40048.